

WaterMax: breaking the LLM watermark detectability-robustness-quality trade-off

Eva Giboulot¹ Teddy Furon¹

Abstract

Watermarking is a technical means to dissuade malfeasant usage of Large Language Models. This paper proposes a novel watermarking scheme, so-called WaterMax, that enjoys high detectability while sustaining the quality of the generated text of the original LLM. Its new design leaves the LLM untouched (no modification of the weights, logits, temperature, or sampling technique). WaterMax balances robustness and complexity contrary to the watermarking techniques of the literature inherently provoking a trade-off between quality and robustness. Its performance is both theoretically proven and experimentally validated. It outperforms all the SotA techniques under the most complete benchmark suite.

1. Introduction

The availability of powerful large-language models (LLMs) allows users to produce texts that look like human writings. The risk for misuse of these models is critical, ranging from the impersonation of individuals to the large-scale generation of fake news. Identifying the provenance of a given piece of text is paramount to limit the impact of such ‘weaponization’ of LLMs. New initiatives or regulations impose technical means for AI traceability (NIST, 2023; EUParliament, 2023; CAC, 2022).

There exists two main classes of methods to perform such identification: passive methods, i.e., forensics, and active methods, i.e., watermarking. Forensics methods for generated texts generally leverage a priori knowledge about the statistics of texts generated by a given class of LLMs (Wu et al., 2023; Mitchell et al., 2023). Despite their versatility, these methods offer lower performance than watermarking and do not provide strong guarantees on false alarm rates. The reported probabilities are only validated empirically on some datasets, and because of this, they are never lower than

*Equal contribution ¹Univ. Rennes, Inria, CNRS, IRISA, France. Correspondence to: <eva.giboulot@inria.fr>.

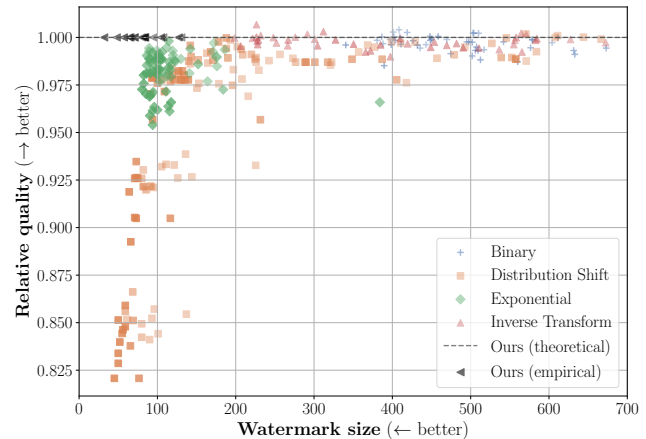


Figure 1: The relative quality of the watermarked text as a function of the watermark size (*i.e.* the number of tokens necessary to detect the watermark - see definitions in Sect. 7). Transparency indicates a less robust scheme. Our watermark attains a small watermark size without losing quality.¹.

10^{-3} (Hans et al., 2024).

In contrast, active methods are only limited by the fact the LLM owner must integrate the watermarking within the generation processes. This is done by embedding an imperceptible signal in the generated text, which can be retrieved by a detector sharing the secret key of the model owner. Current watermarking methods for generative texts (Kirchenbauer et al., 2023b; Aaronson & Kirchner, 2023; Kudipudi et al., 2023; Christ et al., 2023) have shown to lead to extremely high detection rates with an acceptable impact on text quality. Despite that, they are all prone to the same limitations described in Section 2.

This paper presents WaterMax, a new watermarking technique for LLM-generated text. It obeys the regular constraints found in the literature: it can be integrated into any standard LLM without fine-tuning the weights, the detection does not need the original LLM, and it can spot the watermark on a slice of generated text with some guarantee on the false alarm rate. Our contributions are the following:

¹The figure is adapted from Fig. 5 of (Piet et al., 2023) with values graciously shared by the authors – except for our scheme.

- Our scheme improves a lot the quality of the generated text as well as the detectability of the watermark. Fig. 1 clearly shows that the other methods need to boost the watermark strength to become detectable on short texts, inevitably degrading the quality, whereas our scheme sustains a pristine quality of the generated text.
- Our design is new. The high text quality comes from the fact that it does not rely on the usual mechanisms of the literature, especially it keeps the next token distribution, the sampling temperature and technique intact. Moreover, it better utilizes the text entropy by working over sub-sequences of tokens, so-called chunks hereafter, rather than token by token.
- Our study provides a theoretical model of the watermark performance characterizing the false positive and the true positive rates even under attack.

2. Related Work

Watermarking texts generated by LLMs is mainly performed by changing either the sampling distribution of tokens (Kirchenbauer et al., 2023a) or directly the method of selecting the next token (Aaronson & Kirchner, 2023; Kuditiipudi et al., 2023; Christ et al., 2023). Critically, the false-positive rate of these methods can be reliably controlled (Fernandez et al., 2023). Furthermore, the computational cost of most of these methods is negligible relative to the text generation itself.

On the other hand, they all suffer from similar weaknesses:

Token entropy limit Recent theoretical works (Christ et al., 2023; Huang et al., 2023; Kirchenbauer et al., 2023a; Aaronson & Kirchner, 2023) show that the watermark detectability is highly dependent on the entropy of the next token distribution at each step. In practice, this makes the text length necessary for a reliable watermark detectability dependent on the type of text. One solution is to adapt the temperature in the LLM to increase the entropy artificially (Idrissi et al., 2023; Liu & Bu, 2024).

Quality of the generated text Kuditiipudi et al. (2023) claim that a watermark is distortion-free provided it does not modify the probability distribution of the next token *on average* over the keys. This is guaranteed, for instance, in schemes like (Aaronson & Kirchner, 2023; Kuditiipudi et al., 2023; Christ et al., 2023). However, as shown in (Piet et al., 2023), this does not lead to a better watermarking scheme in practice, as individual texts still incur a non-negligible distortion. Other techniques like (Kirchenbauer et al., 2023a) modify the probability distribution of the next token, and it is not straightforward to predict the impact on the quality. In practice, there is a trade-off between text quality and wa-

termark strength, with more detectable watermarks leading to significant text degradation (Fernandez et al., 2023; Piet et al., 2023).

Text size limit All these schemes are based on a score function that accumulates watermarking evidences over individual tokens. Consequently, their power is an increasing function of the text size, with small texts being more difficult to watermark without losing quality.

Our new watermarking method addresses all these problems. In particular, our scheme can theoretically reach an arbitrary watermarking power without any loss in text quality, even for short texts given enough entropy. This is done by directly minimizing the p -value of a full text for a watermark detector instead of performing an ad-hoc manipulation of individual tokens. This method has a computational cost, which we show how to limit throughout the paper.

Watermark robustness characterization The watermarking signal must resist different types of text editing, ranging from a simple insertion of new words to a complete paraphrasing of the text. At the time of writing, there is a single watermarking scheme designed from the ground up to be robust (Kuditiipudi et al., 2023) – the "Inverse Transform" scheme in 1. Despite that, other state-of-the-art methods have experimentally shown resiliency to attacks against long-form texts (Piet et al., 2023) with much better performance in detectability. They ensure a precise control of the false-positive rate (Fernandez et al., 2023). However, none of these methods can theoretically guarantee the detector's power. Only bounds on the moments of the detection score are provided in (Kirchenbauer et al., 2023a) and (Aaronson & Kirchner, 2023).

In contrast, Section 5 completely characterizes our scheme's performance under a large attack range by expressing both false-alarm and true-positive rates.

3. Watermarking by generating multiple texts

This section presents a simplified and inefficient version of the final algorithm for a pedagogical purpose.

3.1. Main Idea

The driving idea is that a LLM is a randomized algorithm. In its simplest implementation, the LLM computes a probability distribution of the next token and *randomly* samples according to this distribution. The chosen token is appended to the context, and the process iterates. This implies that the output text may differ when submitting the same prompt several times. Our main idea is to let the LLM generate several texts and select the one that is the most suitable from the watermarking point of view.

Initially, we select a watermark detection algorithm that is sound in the sense that it can output a p -value for any piece of text under scrutiny. Usually, such detection computes a score and then ‘normalizes’ it in a p -value defined as the probability that a non-watermarked text yields a score equal to or higher. The p -value is uniformly distributed over $[0, 1]$ if the text under scrutiny is not watermarked; otherwise, the p -value takes a small value. Appendix A lists some candidates from the literature and presents our design used for the experiments.

Our proposed watermark embedding lets the LLM generate n texts for a given prompt. Each text is produced normally using any sampling technique, be it a variant of nucleus sampling or beam search. Since all pieces of text are generated normally, *i.e.* without being degraded by a watermark, their qualities are likely high. From the n generated texts, the LLM outputs the text with the lowest p -value.

We suppose for the moment that a text is deemed watermarked if its p -value evaluated by the very same detection algorithm is lower than the required false alarm probability P_{FA} . This raises the question of the number n of generated texts for successfully embedding the watermark.

The main advantage of this procedure is that the watermark does not degrade the quality of the text and that any detection procedure may be used, provided it is sound. The price to pay is high complexity and long latency. Section 4 shows a simple way to solve this issue. Before that, the sequel formalizes this simple idea.

3.2. Formalization

The main ingredient of our scheme is a watermark detection that outputs a p -value for any text input, whatever its length. This is the case for the main works in the literature, like (Aaronson & Kirchner, 2023; Kirchenbauer et al., 2023a; Christ et al., 2023) and to some extent (Kuditipudi et al., 2023) (see App. A). Of note, the computation of the p -value can be hazardous on texts with repetitions of token subsequences and Fernandez et al. (2023) indicate how to fix this issue. This means that the p -value P computed from a random non-watermarked text is uniformly distributed over $[0, 1]$ with p.d.f. $f(p|\mathcal{H}_0) = \mathbb{1}_{[0,1]}(p)$.

For a given prompt, the generator creates n independent texts, each with possibly a different number of tokens, computes their p -values $P_j \stackrel{\text{iid}}{\sim} \mathcal{U}_{[0,1]}$, and outputs the text with the minimum p -value. A well-known results in statistics states that the minimum of n independent p -values follow a beta distribution $B(1, n)$ whose p.d.f. is $f(p|\mathcal{H}_1) = n(1-p)^{n-1}$.

The detector receives an unknown text and decides between two hypotheses:

- \mathcal{H}_0 : The text is not watermarked. The p -value has not been ‘minimized’ and follows the uniform distribution.
- \mathcal{H}_1 : The text is watermarked. Assuming no attack was performed, the p -value is distributed as a minimum of n independent uniform variables. We assume the detector knows the value of n .

Since the distributions under both hypotheses are known, the detector performs a simple test, and the Neyman-Pearson lemma states that the most powerful test under a given probability of false-alarm P_{FA} is the (log) likelihood-ratio test:

$$\Lambda(p) \triangleq \log \left(\frac{f(p|\mathcal{H}_1)}{f(p|\mathcal{H}_0)} \right) \stackrel{\mathcal{H}_0}{\leq} \tau, \quad (1)$$

where τ is a threshold which depends on P_{FA} . In our setting, $\Lambda(p) = (n-1)\log(1-p) + \log(n)$, which is a monotonic function of p . In other words, comparing $p \stackrel{\mathcal{H}_1}{\leq} P_{FA}$ is equivalent to the Neyman-Pearson test. The power of the test is defined as the probability of detecting a watermarked text and turns out to be an increasing function w.r.t. n :

$$P_D \triangleq \mathbb{P}(P < P_{FA}|\mathcal{H}_1) = 1 - (1 - P_{FA})^n. \quad (2)$$

We point the reader to two important advantages:

- The performance of the test does not depend on the choice of the detection scheme.
- The performance of the test does not depend on the length of the text. Consequently, even an extremely small text can be watermarked in theory.

Figure 2 plots the power of the test as a function of n for various probabilities of false alarm. Whatever the choice of P_{FA} , one can clearly observe that a huge number of generated texts ($\gg 50$) is required to obtain a power greater than 0.5, which is unacceptable in practice. Section 4 shows how to improve this base algorithm to reach arbitrarily high power with a smaller cost in terms of computational power.

Another weakness is the assumption that the LLM can create n texts whose p -values are independent. For some prompts, the diversity (*i.e.* entropy) is indeed small, which implies that the LLM creates similar texts or even duplicates of text among the n outputs. Section 6 investigates how self-synchronization mitigates this issue.

4. Watermarking chunks of text

This section devises ways to efficiently explore the space of possible texts to find a low p -value. The main idea is to split the generation into N iterations, each iteration creating a chunk of the text. For each chunk, a batch of n text drafts

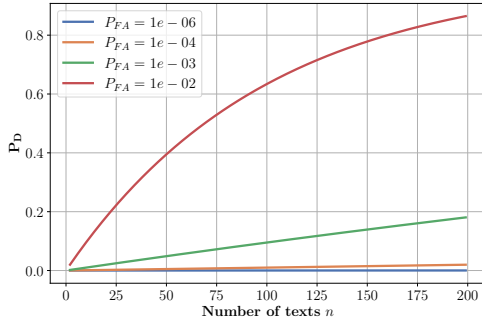


Figure 2: Theoretical power of the uniformly most powerful test (2) as a function of the number of generated texts n for different probability of false-alarm.

is generated independently based on the text candidates of the previous iteration. This allows us to reduce the computational burden by generating only small chunks of text at each iteration while exploring many possible texts. We choose a Viterbi-like algorithm among several exploration strategies ranging from greedy search to Monte Carlo Tree Search (Chaffin et al., 2022).

4.1. Exploring the text space

Ideally, one would generate n drafts at each chunk for each previous candidate, resulting in a tree of n^N texts from which to choose the lowest p -value. Obviously, this is not computationally feasible. We reduce the complexity by keeping only the m best candidates at each step, akin to a beam-search or a Viterbi algorithm (Viterbi, 1967). This is suboptimal because the candidates minimizing the p -value at a given step may not be the best once completed at iteration N . The pseudo-code is summarized in Alg. 1.

4.2. Cumulative scores

This paper considers detection schemes that share the following process. The vocabulary \mathcal{V} is a list of $|\mathcal{V}|$ admissible tokens, and a text is decomposed into a sequence of L tokens. Depending on the secret key k , the detection associates to the i -th token a variable u_i . The score is computed as the sum over the tokens $s = \sum_{i=1}^L u_i$. This is translated into a p -value assuming that, under \mathcal{H}_0 , i) the scores of the tokens are independent and identically distributed random variables $(U_i)_{i=1}^L$, giving birth to a random score S , ii) whose c.d.f. $F_S(\cdot; L)$ is known so that the p -value is simply:

$$p = \mathbb{P}(S > s) = 1 - F_S(s; L). \quad (3)$$

Appendix A lists some detection schemes of the literature following this procedure. Our choice is simply $U_i \stackrel{\text{iid}}{\sim} \mathcal{N}(0; 1)$ so that $F_S(s; L) = \Phi(s/\sqrt{L})$.

Algorithm 1 Iterative watermarking of generated texts

Input: prompt pr , parameters (N, n, m, ℓ) , p -value computation Detect, LLM Generate

Initialize: $\mathbf{x}_j = \emptyset, \forall 1 \leq j \leq m$

for $i = 1$ **to** N **do**

for $j = 1$ **to** m **do**

 context = $[pr \parallel \mathbf{x}_j]$

for $k = 1$ **to** n **do**

$\nu = n(j-1) + k$

$\mathbf{y}_\nu = \text{Generate}(\text{context}, \ell)$

$p_\nu = \text{Detect}([\mathbf{x}_j \parallel \mathbf{y}_\nu])$

end for

end for

$(\nu_1, \dots, \nu_m) = \arg \min_{1 \leq \nu \leq mn} p_\nu$

for $j = 1$ **to** m **do**

$\mathbf{x}_j = [\mathbf{x}_{\lfloor \nu_j/n \rfloor + 1} \parallel \mathbf{y}_{\nu_j}]$

end for

end for

$l = \arg \min_{1 \leq j \leq m} \text{Detect}(\mathbf{x}_j)$

Output: \mathbf{x}_l

For the sake of clarity, suppose that the chunks are composed of ℓ tokens. At iteration i , the j -th candidate has a score denoted $s_{i,j}$ and n drafts for its following chunk are proposed. This produces n incremented scores per candidate, thus mn variables: $s_{i,j} + \delta s_{i,j,k}$, $1 \leq j \leq m$, $1 \leq k \leq n$. Since these scores are converted into p -values by the same function, *i.e.* $p = 1 - F_S(s; \ell(i+1))$, selecting the m lowest p -values amounts to keep the m candidates maximizing the cumulative scores, hence the name of our scheme: WaterMax.

4.3. Low latency

Another issue is the latency: the final text cannot be issued until all candidates reach an end of sequence. This problem is fixed with the drastic choice $m = 1$. It amounts to a greedy search appending to the text at iteration i the chunk draft yielding the biggest incremental score $\delta s_{i,1,k}$. This choice enables the output of a chunk of text at the end of each iteration, hence reducing latency. Of note, this also corresponds to the draft with the lowest local p -value $1 - F_S(\delta s_{i,1,k}; \ell)$.

4.4. Optimal detection without attack

This section introduces a simple detector to reveal the advantage of our watermark embedding. The idea is that the received text is composed of chunks whose local p -values are distributed as beta distributions $B(1, 1)$ (*i.e.* $\mathcal{U}_{[0,1]}$) under \mathcal{H}_0 or $B(1, n)$ under \mathcal{H}_1 (see Sect. 3.2). This is a generalization of the algorithm of the previous section, the only difference being that the likelihood ratio (1) now aggregates

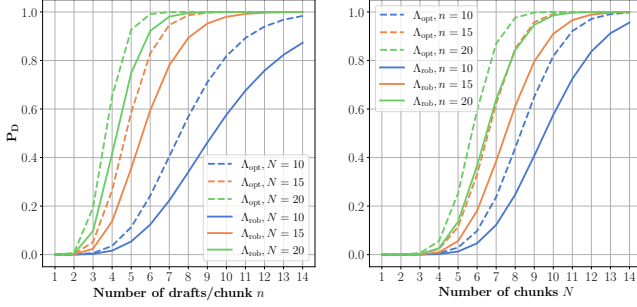


Figure 3: Theoretical power of the optimal (4) and robust 7 tests at $P_{FA} = 10^{-6}$ for $m = 1$ as a function of the number of drafts n per chunk and the number of chunks N .

a vector \mathbf{p} of N observed local p -values:

$$\Lambda_{\text{opt}}(\mathbf{p}) = -\sum_{i=1}^N \log(1 - p_i) \stackrel{\mathcal{H}_0}{\leq} \tau. \quad (4)$$

Proposition 4.1. *The optimal detector Λ_{opt} has the following test’s performance when there is no attack:*

$$P_{FA} = \gamma_{N,1}(\tau), \quad (5)$$

$$P_D = \gamma_{N, \frac{1}{n}}\left(\gamma_{N,1}^{-1}(P_{FA})\right). \quad (6)$$

where $\gamma_{x,y}$ is the lowest incomplete gamma function with shape parameter x and scale parameter y .

Appendix B gives a sketch of the proof.

Again, notice that neither the distribution of the token variables nor the length of the chunks plays a role in the test performance (with the important caveat that a chunk must not be empty). Figure 3 illustrates the major impact of the number of chunks. Contrary to Sect. 3, we can easily reach a power close to 1 even at $P_{FA} = 10^{-6}$. For example, using $N = 9$ chunks of $n = 15$ drafts, assuming a medium-size text of $L = 512$ tokens and chunks of equal length, one only needs to generate $Nn = 135$ chunk drafts of $\ell = \lceil L/N \rceil = 57$ tokens to obtain a power of 0.96. This is equivalent to generating 15 texts of size 512. This is to compare to Sect. 3 where more than 3 million texts of 512 tokens are necessary to reach this power at $P_{FA} = 10^{-6}$.

5. Robust watermark detection

Until this point, our detector assumed that the text it receives is the generated text. In other words, the model of the previous section does not consider possible attacks. Indeed, before reaching the detector, a text might have been modified for legitimate or malicious reasons: it may be translated, curated, locally modified *etc.*

5.1. Robust detection

Detector (4) is neither optimal nor robust under attack because the insertion or the removal of tokens provokes a desynchronization: The detector no longer knows where each chunk starts and ends, which is necessary for computing the local p -value of individual chunks. More robustness comes with a global score summing up over all the tokens:

$$\Lambda_{\text{rob}}(\mathbf{u}) = \sum_{i=1}^N \sum_{j=1}^{\ell} u_{(i-1)\ell+j}. \quad (7)$$

Proposition 5.1. *The robust detector has the following test performance when there is no noise:*

$$P_{FA} = \Phi(-\tau/\sqrt{L}), \quad (8)$$

$$P_D \approx \Phi\left(\frac{\Phi^{-1}(P_{FA}) + \sqrt{N}e(n)}{\sqrt{v(n)}}\right). \quad (9)$$

Appendix C gives a sketch of the proof.

The robust test (7) is less powerful than (4) when there is no attack. Figure 3 shows that the robust test (7) is slightly less powerful than the optimal test (4) when there is no attack. The following section shows that its power degrades smoothly in case of token insertion or removal.

5.2. A model of the robustness against attack

Despite the variety of modifications that can be performed on a watermarked text, all attacks have the same end effect: modifying the tokens and potentially the number of tokens. This amounts to modifying a proportion of the token variables to be distributed following \mathcal{H}_0 instead of \mathcal{H}_1 in the global score. Formally, the score $\Lambda_{\text{rob}}(\mathbf{U})$ for a text of L tokens becomes: (assuming αL is an integer)

$$\Lambda_{\text{rob}}(\mathbf{U}) = \sum_{i=1}^{\alpha L} U_{\pi_0(i)} + \sum_{i=1}^{(1-\alpha)L} \bar{U}_{\pi_1(i)}, \quad (10)$$

where $1 - \alpha$ is the proportion of modified tokens whose variables are denoted $\{\bar{U}_i\}$, and π_0 (resp. π_1) is mapping to the indices of the untouched tokens (resp. modified tokens). It is important to note that it does not matter if the attacked text’s size differs from the generated text’s size.

It is clear that $\bar{U}_i \stackrel{\text{iid}}{\sim} \mathcal{N}(0; 1)$. However, Appendix D shows that $\Lambda_{\text{rob}}(\mathbf{U})$ is *not* distributed as $\alpha S_1 + (1 - \alpha)S_0$ where S_i is the score under \mathcal{H}_i .

Proposition 5.2. *The robust detector has the following test performance under attack:*

$$P_{FA} = \Phi(-\tau/\sqrt{L}), \quad (11)$$

$$P_D \approx \Phi\left(\frac{\Phi^{-1}(P_{FA}) + \alpha\sqrt{N}e(n)}{\sqrt{1 + \alpha^2(v(n) - 1)}}\right). \quad (12)$$

Appendix D gives a sketch of the proof.

In the end, the power of the test decreases smoothly with the strength $(1 - \alpha)$ of the attack. Observe that, once again, the power of the test does not depend on the size of the text.

6. Independence

This section discusses the major assumptions made so far.

6.1. Token variable independence

All random variables (U_i) associated with tokens must be independent and identically distributed within a text. This assumption has an impact on the power of the test and especially on the probability of false alarm. It must hold for non-watermarked text. Otherwise, the score of a chunk (or of a full text) is not properly normalized into a p -value.

We use the exact same technique as in (Fernandez et al., 2023) to enforce the token variable independence: the variable U_i of the i -th token of a text depends not only on the secret key but also on the hashing of the current token and the $h - 1$ previous token of the text (a window of size h). Furthermore, this h -gram is appended to a list. If the h -gram is already stored in that list, its variable is discarded for computing the score. By discarding identical h -grams, we ensure that for a given text, the (U_i) are always different. Contrary to (Fernandez et al., 2023), this mechanism is enforced during both the generation and the detection phases to ensure that both sides compute the same score.

6.2. Draft score independence

At the embedding, the scores of the n drafts of a chunk should be independent. Correlations occur when parts of texts repeat across different drafts. For example, in a prompt asking "Who are you?", it is likely that many drafts of the first chunk of the response start by "I am". This assumption only plays a role in the power of the detector.

The inter-draft independence is tackled using the same methods. Note that the longer the window, the more likely a h -gram is new and the more diverse the scores. Yet, this diversity is obtained at the cost of robustness. Indeed, changing a single token in a text removes the watermark of h tokens because their variables depend on the modification. One case guarantees draft score independence: when beam-search generates drafts instead of sampling (thus ensuring n different texts) and the whole draft is hashed for seeding each variable token. Sadly, this creates a watermark that breaks even for a single modified token. *This forces us to use a causal window*, meaning that the score of each token depends only on itself and the previous tokens. This has an important weakness: at a given iteration, the j -th token ($j < h$) of every draft always refers to the same $h - j$

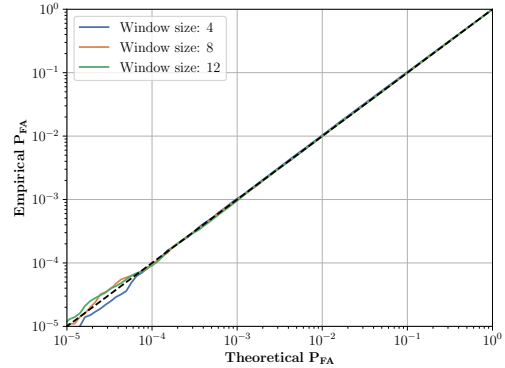


Figure 4: Empirical P_{FA} as a function of the theoretical P_{FA} for Λ_{opt} on $10 \times 100k$ Wikipedia entries truncated at 256 tokens. Both quantities match whatever the window size h for the hash, demonstrating the token variable independence.

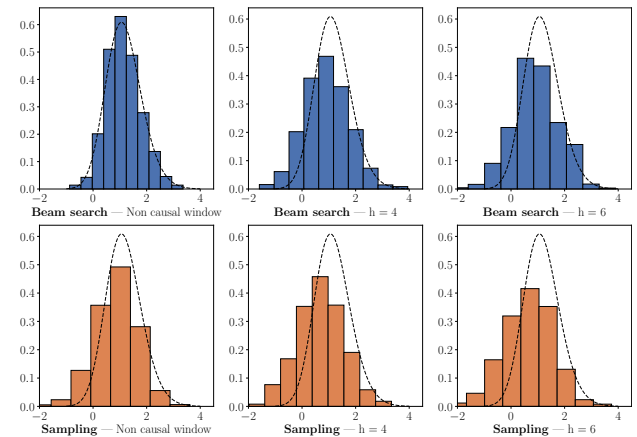


Figure 5: Histograms of watermark scores for $N = 16$ chunks and $n = 5$ drafts. The black curve is the theoretical p.d.f.

tokens since the previous chunk is identical for all these drafts. This means that the effective window size for this token is always smaller than h . In summary, we cannot guarantee our watermarking scheme perfectly adheres to this assumption while also being robust to attacks.

6.3. Experimental validation

For the independence of the token variables, the experiment runs the detector on 100k Wikipedia entries from 2018 for ten different keys. Since the text of Wikipedia is free of any watermark, one should observe p -values uniformly distributed, *i.e.* the empirical false alarm rate should match the theoretical probability of false alarm. Figure 4 demonstrates that this assumption holds for any window size h . On the other hand, the tamper resistance highly depends on the hashing window size, with $h = 4$ being a good trade-off between performance and robustness.

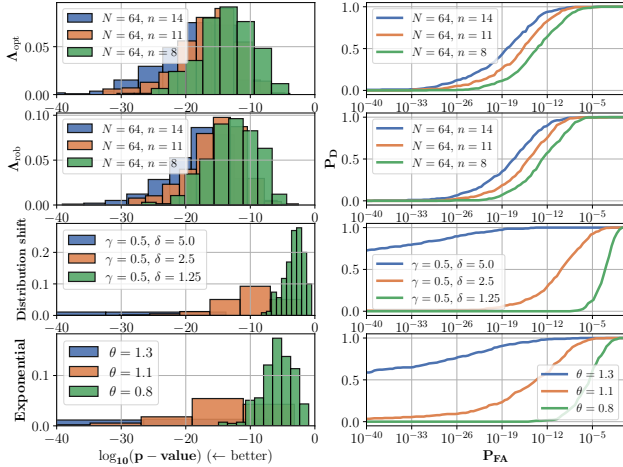


Figure 6: Detectability of WaterMax (optimal and robust), ‘distribution shift’, and ‘exponential’ without attack. (Left) histogram of p -values, (Right) ROC curve.

The second experiment measures how much we deviate from the draft score independence. It generates 100 texts of 128 tokens on the “fake news” task from (Piet et al., 2023). The entropy of the generated texts may be low for a given chunk so that some parts of a text may be redundant among the drafts. Figure 5 reports how much our scores under \mathcal{H}_1 deviate from the theoretical distribution.

First, our theoretical model perfectly matches the empirical distribution when we use beam search and a non-causal window. This is expected since this setup guarantees the draft score independence if at least one token differs between the drafts. On the other hand, a causal window, whatever its size h , provokes a mismatch with the theory. Interestingly, the empirical distribution is close to the theoretical distribution for fewer drafts per chunk: the redundancy within the drafts makes a smaller “effective” n . Note that the impact is limited. Figure 3 shows that n slightly weakens the test’s power compared to the number of chunks N . The watermark remains highly detectable as long as N is large because the draft score dependence impacts only n ,

7. Experiments

7.1. Metrics

The evaluation of a watermarking scheme is based on three quantities: 1) the quality of the watermarked text relative to the non-watermarked text, 2) the detectability of the watermark, and 3) its robustness against attacks.

Text quality Two metrics evaluate the quality of watermarked text: 1) the rating given by Llama2 when prompted to evaluate the text as proposed by Piet et al. (2023) in their Mark My Words (MMW) benchmark and 2) the measure of perplexity proposed by Kirchenbauer et al. (2023a)

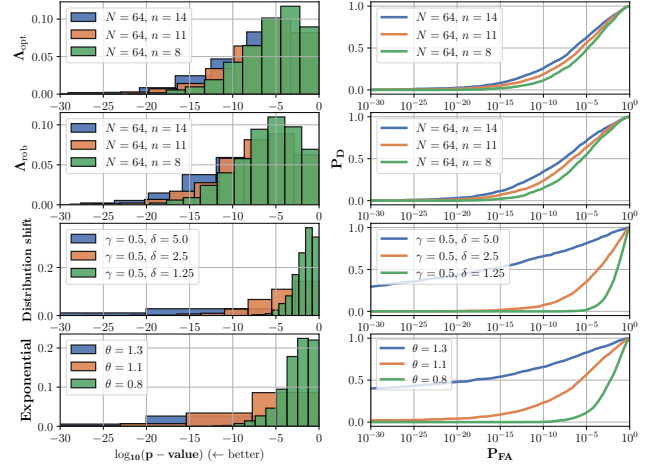


Figure 7: Detectability of WaterMax (optimal and robust), ‘distribution shift’ and ‘exponential’ with the MMW suite of attacks. (Left) histogram of p -values, (Right) ROC curve.

using OPT-2.7b (Zhang et al., 2022) on the newslake C4 dataset (Raffel et al., 2020).

Detectability Piet et al. (2023) measure watermark detectability by the *watermark size* defined in MMW. This is the median number of tokens necessary to detect the watermark at $P_{FA} = 0.02$. We also report the p -values and ROC curves for each benchmarked dataset in Figure 6-7.

Robustness The MMW benchmark is the first to propose a full suite of attacks on the watermarked texts, including swap (remove, add, or swap words), replacement with synonym, paraphrasing, translation, contraction, expansion, lower case, misspelling, and typos addition. See (Piet et al., 2023) for details. The measure, named *tamper resistance*, aggregates these results.

All quantities related to the MMW benchmark are measured with the code provided by the authors².

7.2. State-of-the-art methods

The benchmark MMW considers four techniques names as ‘binary’ (Christ et al., 2023), ‘distribution shift’ (Kirchenbauer et al., 2023a), ‘exponential’ (Aaronson & Kirchner, 2023), ‘inverse transform’ (Kuditipudi et al., 2023). It concludes that today’s best methods are ‘distribution shift’ and ‘exponential’. This is visible in Fig. 1 where these two methods are the only ones approaching the upper left corner. We set the green-list ratio of ‘distribution shift’ to $\gamma = 0.5$ following the recommendation of Piet et al. (2023).

All the evaluations use Llama2-7b-chat (Touvron et al., 2023) with temperature $T = 1$. The length of a chunk ℓ is fixed *a priori* to L/N where L is the maximum number

²github.com/wagner-group/MarkMyWords

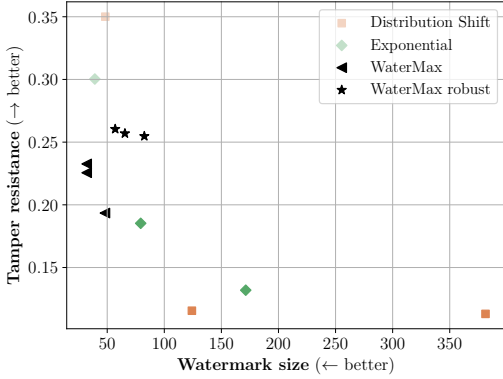


Figure 8: Tamper resistance as function of watermark size at $P_{FA} = 0.02$. The configurations leading to a relative quality of less than 0.9 and relative perplexity less than 0.8 are shown transparent. The values presented here correspond to the configurations of the watermarks in Figure 6.

of tokens allowed in the benchmark (1024 for MMW and 200 for C4) and N the number of chunks. The LLM may generate texts shorter than L tokens, leading to less than N chunks, and the last chunk may not have ℓ tokens exactly. Except when specified otherwise, the watermark methods all use a window size of 4 for hashing.

7.3. Results

Figure 1 summarizes the Mark My Words benchmark outcomes. They confirm that WaterMax produces detectable watermarked texts whose quality matches the one of the original LLM output, even for a small watermark size as low as 32 tokens (with $(N, n) = (64, 14)$). Figure 9 draws similar conclusions. The perplexity increases slowly but tends to stay close to the original one, whatever the detectability of the watermark. This is in stark contrast to ‘distribution shift’ reaching lower p -values at the cost of a greatly increased perplexity. Importantly, the relative perplexity of ‘exponential’ fastly degrades since one modifies the sampling temperature to vary the watermark strength.

A close look at Fig. 6 validates the greater impact of the number of chunks N compared to the number of drafts n . Indeed, with $N = 64$ for MMW, we reach a power close to 1 at $P_{FA} = 10^{-10}$ at virtually no quality loss for $n \in (8, 14)$. In comparison, ‘distribution shift’ at $\delta = 0.25$ has an equivalent power for $P_{FA} = 10^{-4}$, yet at a higher cost to both perplexity and Llama2 rating.

The robust detector Λ_{rob} loses almost no power compared to Λ_{opt} when no attack is performed, while being more robust against the MMW attack suite, see Figure 7. Furthermore, our scheme also reaches higher tamper-resistance than other watermark with similar quality as shown in Fig. 8. Theoretically, Eq. (12) tells that we can reach an arbitrary high tamper-resistance by increasing the number of chunks. This

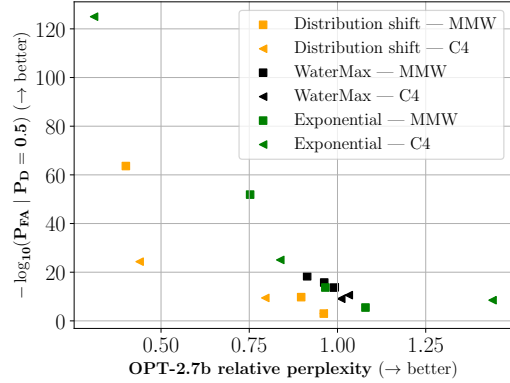


Figure 9: Median of the $\log_{10} p$ -value as a function of the relative perplexity measured by the oracle model OPT-2.7b. The relative perplexity is computed on texts having the same size $\pm 10\%$. The values presented here correspond to the configurations of the watermarks in Figure 6

should compensate for a small α , *i.e.* a strong attack. Yet, the computational cost of doing may become prohibitive: WaterMax strikes a trade-off between complexity and robustness when the other schemes trades either quality or watermark size for robustness. All their configurations maximizing tamper-resistance in Fig. 8 lead to a tangible loss of quality (relative quality lower than 0.9, relative perplexity lower than 0.8).

7.4. Computational complexity

At face value, the computational cost of our scheme is nothing more than Nn text generations, the computation of the scores being negligible. However, the cost of adding one more chunk is higher than the cost of generating one more draft. Indeed, the n drafts of a chunk are sampled independently (or by a beam search), making their computation highly parallelizable on modern GPUs. On the other hand, we cannot parallelize the computations over the chunk. Since N has the highest impact on the power of WaterMax, it is the main limiting factor for its performance. See Appendix E for experimental running times.

8. Conclusion

Contrary to previous art, the design of WaterMax starts from a detector and then constructs the generator to maximize the detection power. Consequently, this watermark enjoys several appealing properties: it reaches both high quality and robustness even on short texts and it does not modify any component of the LLM in any way. This is at the cost of computational complexity, which stays limited thanks to the parallelization possibilities of modern GPUs. This design complies with common tricks in the literature, like adapting the sampling temperature (Idrissi et al., 2023) or embedding short messages (Fernandez et al., 2023).

9. Impact statement

This paper presents work whose goal is to improve methods for the identification of texts generated by LLMs. Societal consequences are mainly beneficial, increasing the transparency and traceability of AI as required in recent legislations (NIST, 2023; EUParliament, 2023; CAC, 2022).

References

- Aaronson, S. and Kirchner, H. Watermarking GPT outputs, 2023. URL <https://scottaaronson.blog/?m=202302>.
- CAC. Cyberspace Administration of China: Provisions on the administration of deep synthesis internet information services, 2022. URL <https://www.chinalawtranslate.com/en/deep-synthesis/>.
- Chaffin, A., Claveau, V., and Kijak, E. PPL-MCTS: constrained textual generation through discriminator-guided MCTS decoding. In Carpuat, M., de Marneffe, M., and Ruíz, I. V. M. (eds.), *Proceedings of the 2022 Conference of the North American Chapter of the Association for Computational Linguistics: Human Language Technologies, NAACL 2022, Seattle, WA, United States, July 10-15, 2022*, pp. 2953–2967. Association for Computational Linguistics, 2022. URL <https://aclanthology.org/2022.naacl-main.215>.
- Christ, M., Gunn, S., and Zamir, O. Undetectable watermarks for language models. *Cryptology ePrint Archive, Paper 2023/763*, 2023. URL <https://eprint.iacr.org/2023/763>.
- EUParliament. EU AI Act: first regulation on artificial intelligence, 2023. URL <https://www.europarl.europa.eu/news/en/headlines/society/20230601STO93804/eu-ai-act-first-regulation-on-artificial-intelligence>.
- Fernandez, P., Chaffin, A., Tit, K., Chappelier, V., and Furon, T. Three bricks to consolidate watermarks for Large Language Models. *2023 IEEE International Workshop on Information Forensics and Security (WIFS)*, 2023.
- Hans, A., Schwarzschild, A., Cherepanova, V., Kazemi, H., Saha, A., Goldblum, M., Geiping, J., and Goldstein, T. Spotting LLMs with binoculars: Zero-shot detection of machine-generated text, 2024.
- Huang, B., Zhu, B., Zhu, H., Lee, J. D., Jiao, J., and Jordan, M. I. Towards optimal statistical watermarking, 2023.
- Idrissi, B. Y., Millunzi, M., Sorrenti, A., Baraldi, L., and Dementieva, D. Temperature matters: Enhancing watermark robustness against paraphrasing attacks. 2023.
- Kirchenbauer, J., Geiping, J., Wen, Y., Katz, J., Miers, I., and Goldstein, T. A watermark for Large Language Models. *arXiv preprint arXiv:2301.10226*, 2023a.
- Kirchenbauer, J., Geiping, J., Wen, Y., Shu, M., Saifullah, K., Kong, K., Fernando, K., Saha, A., Goldblum, M., and Goldstein, T. On the reliability of watermarks for Large Language Models, 2023b.
- Kuditipudi, R., Thickstun, J., Hashimoto, T., and Liang, P. Robust distortion-free watermarks for language models. *arXiv preprint arXiv:2307.15593*, 2023.
- Liu, Y. and Bu, Y. Adaptive text watermark for Large Language Models, 2024.
- Mitchell, E., Lee, Y., Khazatsky, A., Manning, C. D., and Finn, C. DetectGPT: zero-shot machine-generated text detection using probability curvature, 2023.
- NIST. National Institute of Standards and Technology: Calls for information to support safe, secure and trustworthy development and use of artificial intelligence, 2023. URL <https://www.nist.gov/news-events/news/2023/12/nist-calls-information-support-safe-secure-and-trustworthy-development-and>.
- Piet, J., Sitawarin, C., Fang, V., Mu, N., and Wagner, D. Mark My Words: analyzing and evaluating language model watermarks. *arXiv preprint arXiv:2312.00273*, 2023.
- Pillutla, K., Swayamdipta, S., Zellers, R., Thickstun, J., Welleck, S., Choi, Y., and Harchaoui, Z. Mauve: Measuring the gap between neural text and human text using divergence frontiers. *Advances in Neural Information Processing Systems*, 34:4816–4828, 2021.
- Raffel, C., Shazeer, N., Roberts, A., Lee, K., Narang, S., Matena, M., Zhou, Y., Li, W., and Liu, P. J. Exploring the limits of transfer learning with a unified text-to-text transformer. *The Journal of Machine Learning Research*, 21(1):5485–5551, 2020.
- Touvron, H., Martin, L., Stone, K., Albert, P., Almahairi, A., Babaei, Y., Bashlykov, N., Batra, S., Bhargava, P., Bhosale, S., et al. Llama 2: Open foundation and fine-tuned chat models. *arXiv preprint arXiv:2307.09288*, 2023.
- Viterbi, A. Error bounds for convolutional codes and an asymptotically optimum decoding algorithm. *IEEE Transactions on Information Theory*, 13(2):260–269, 1967. doi: 10.1109/TIT.1967.1054010.

- Wu, K., Pang, L., Shen, H., Cheng, X., and Chua, T.-S. LLMdet: a third party Large Language Models generated text detection tool. In *Findings of the Association for Computational Linguistics: EMNLP 2023*, pp. 2113–2133, 2023.
- Zhang, S., Roller, S., Goyal, N., Artetxe, M., Chen, M., Chen, S., Dewan, C., Diab, M., Li, X., Lin, X. V., et al. Opt: Open pre-trained transformer language models. *arXiv preprint arXiv:2205.01068*, 2022.

A. Possible detection schemes

This section describes the detection of the three main LLM watermarking schemes. They share the same process:

- The received text is decomposed into a sequence of, say L , tokens
- A sliding window of size h forwards the selected tokens to a cryptographic function which computes a hash that is xored with the secret key to compose the seed of a Pseudo Random Number Generator
- The variable u_i is computed for the i -th token, $i > h$ based on the output of the PRNG seeded by the h previous tokens
- The score is the sum of the variable: $s = \sum_{i=h+1}^L u_i$
- The score is converted into a p -value: $p = 1 - F_S(s; L)$.

The watermark embedding methods are not detailed because our scheme does not make use of them. This summary is inspired from the work of Fernandez et al. (2023).

For the detection of (Kirchenbauer et al., 2023b), the output of the PRNG is used to create a ‘green’ list which is a subset of \mathcal{V} of size $\gamma|\mathcal{V}|$. Variable U_i is set to 1 if the i -th token belongs to this list, otherwise $U_i = 0$. Therefore, under \mathcal{H}_0 , $U_i \stackrel{\text{iid}}{\sim} \mathcal{B}(\gamma)$ and S follows a binomial distribution $\mathcal{B}(L - h, \gamma)$. This makes

$$p = I_\gamma(s, L - h - s + 1), \quad (13)$$

where I is the regularized incomplete Beta function.

For the detection of (Aaronson & Kirchner, 2023), the output of the PRNG is used to draw $U_i \stackrel{\text{iid}}{\sim} \mathcal{E}(1)$ so that S is Gamma distributed under \mathcal{H}_0 . This makes:

$$p = \frac{\Gamma(L - h, s)}{\Gamma(L - h)}, \quad (14)$$

where Γ is the upper incomplete gamma function. This formulation also holds for (Christ et al., 2023) with the reduction to binary alphabet $|\mathcal{V}| = 2$.

For the detection of (Kuditipudi et al., 2023), the output of the PRNG is used to draw U_i whose distribution matches the distribution of the product of two independent r.v. $\mathcal{U}([-1/2, 1/2])$, i.e. $F_U(u) = 2u(1 - \log(4|u|)) + 1/2$. There is no closed form to turn the global score into a p -value. The authors use either a bound (see Lemma 2.4) or an empirical p -value computed by a costly Monte Carlo simulation with random seeds. This is the reason why this studies fixes the probability of false alarm to a rather large value, i.e. 10^{-2} .

Since Sect. 4.4 shows that the distribution of U_i has no impact, we opt for the simple choice $U_i \stackrel{\text{iid}}{\sim} \mathcal{N}(0, 1)$ and the p -value reads as:

$$p = \Phi\left(-\frac{s}{\sqrt{L}}\right). \quad (15)$$

B. Proof of proposition 4.1

The optimal detector (4) aggregates a vector \mathbf{p} of N observed local p -values:

$$\Lambda_{\text{opt}}(\mathbf{p}) = -\sum_{i=1}^N \log(1 - p_i) \underset{\mathcal{H}_1}{\lesssim} \underset{\mathcal{H}_0}{\gtrsim} \tau. \quad (16)$$

The received text is composed of chunks whose local p -values are distributed as beta distributions $B(1, 1)$ (i.e. $\mathcal{U}_{[0,1]}$) under \mathcal{H}_0 or $B(1, n)$ under \mathcal{H}_1 when there is no attack (see Sect. 3.2). Knowing that if $X \sim B(1, \beta)$ then $-\log(1 - X) \sim \mathcal{E}(\beta)$, $\Lambda(\mathbf{P})$ is the sum of independent exponential r.v. and thus follows a Gamma distribution under both hypothesis but with different parameters:

$$\begin{cases} \Lambda_{\text{opt}}(\mathbf{P}) \sim \Gamma(N, 1) & \text{under } \mathcal{H}_0, \\ \Lambda_{\text{opt}}(\mathbf{P}) \sim \Gamma(N, \frac{1}{n}) & \text{under } \mathcal{H}_1. \end{cases} \quad (17)$$

This leads to the characterization of the test’s performance:

$$P_{FA} = \gamma_{N,1}(\tau), \quad (18)$$

$$P_D = \gamma_{N, \frac{1}{n}}\left(\gamma_{N,1}^{-1}(P_{FA})\right). \quad (19)$$

C. Proof of proposition 5.1

Assume the received text is composed of N chunks of ℓ tokens each so that its total number of tokens $L = N\ell$. Under \mathcal{H}_0 , the token variables are independent and normal distributed so that $\Lambda_{\text{rob}}(\mathbf{U}) \sim \mathcal{N}(0; L)$. It is thus easy to find the threshold τ ensuring a probability of false alarm P_{FA} : $\tau = -\sqrt{L}\Phi^{-1}(P_{FA})$.

Under \mathcal{H}_1 , $\Lambda_{\text{rob}}(\mathbf{U})$ can be written as the sum of N independent chunk scores: $\Lambda_{\text{rob}}(\mathbf{U}) = \sum_{i=1}^N M_i^{(n)}$. These chunk scores are distributed as the maximum of n Gaussian variables $\mathcal{N}(0; \ell)$, corresponding to the score of the drafts. Those maxima have the c.d.f. $F_{M^{(n)}}(x) = \Phi\left(x/\sqrt{\ell}\right)^n$ and one can compute numerically the expectation $\mathbb{E}(M^{(n)}) = \sqrt{\ell}e(n)$ and the variance $\mathbb{V}(M^{(n)}) = \ell v(n)$, see Tab. 1.

An approximation for N large enough is $\Lambda_{\text{rob}}(\mathbf{U}) \sim \mathcal{N}(\mu_1; \sigma_1^2)$ with

$$\mu_1 = N\sqrt{\ell}e(n) = \sqrt{NL}e(n), \quad (20)$$

$$\sigma_1^2 = N\ell v(n) = Lv(n). \quad (21)$$

Table 1: Expectation and variance of the maximum of n independent normal random variables.

| n | 1 | 2 | 3 | 4 | 5 | 6 | 7 | 8 | 9 |
|--------|---|------|------|------|------|------|------|------|------|
| $e(n)$ | 0 | 0.56 | 0.84 | 1.03 | 1.16 | 1.26 | 1.35 | 1.42 | 1.48 |
| $v(n)$ | 1 | 0.68 | 0.56 | 0.49 | 0.45 | 0.42 | 0.40 | 0.37 | 0.36 |

This gives the following power of the test:

$$P_D = \Phi \left(\frac{\Phi^{-1}(P_{FA}) + \sqrt{N}e(n)}{\sqrt{v(n)}} \right). \quad (22)$$

D. Proof of proposition 5.2

This section derives the distribution of *variables of individual tokens* under \mathcal{H}_1 .

We first express the distribution of a vector of L i.i.d. normal variables, given that their sum equals a given value S :

$$\left(\mathbf{U} \mid \sum_{i=0}^L U_i = s \right) \sim \mathcal{N}(S\mathbf{1}_L/L, \mathbf{I}_L - \mathbf{1}_L\mathbf{1}_L^\top/L) \quad (23)$$

with $\mathbf{1}_L$ the vector of all ones in \mathbb{R}^L and \mathbf{I}_L the identity matrix of dimension $L \times L$.

The attacks leaves αL variables untouched (assuming $0 \leq \alpha \leq 1$ and $\alpha L \in \mathbb{N}$). This is encoded in a matrix $\mathbf{A} \in \{0, 1\}^{\alpha L \times L}$ which selects these variables. This means that \mathbf{A} has exactly one single entry equal to 1 in each row, $\mathbf{A}\mathbf{A}^\top = \mathbf{I}_{\alpha L}$, and $\mathbf{A}\mathbf{1}_L = \mathbf{1}_{\alpha L}$.

The sum of these αL variables can be written as $\mathbf{1}_{\alpha L}^\top \mathbf{A}\mathbf{U}$. This makes:

$$\left(\mathbf{1}_{\alpha L}^\top \mathbf{A}\mathbf{U} \mid \sum_{i=0}^L U_i = s \right) \sim \mathcal{N}(\alpha S; L\alpha(1 - \alpha)) \quad (24)$$

This distribution is independent of \mathbf{A} : It does not matter which tokens are left unchanged. For $\alpha = 1$, there is no attack and the variance is null because $\mathbf{1}_{\alpha L}^\top \mathbf{A}\mathbf{U} = \mathbf{1}_L^\top \mathbf{U} = s$. For $\alpha = 0$, the attack has modified all the token variables and the variance is null because $\mathbf{1}_{\alpha L}^\top \mathbf{A}\mathbf{U} = 0$.

According to App. C, an approximation for N large enough is $S \sim \mathcal{N}(\mu_1; \sigma_1^2)$. The law of total variance gives

$$\mathbf{1}_{\alpha L}^\top \mathbf{A}\mathbf{U} \sim \mathcal{N}(\alpha\mu_1; L\alpha(1 - \alpha) + \alpha^2\sigma_1^2). \quad (25)$$

On top of this, the attack adds $(1 - \alpha)L$ tokens distributed under \mathcal{H}_0 , which amounts to add a noise distributed as $\mathcal{N}(0, (1 - \alpha)L)$ to the above score. In the end, the global score is distributed as

$$\Lambda_{\text{rob}}(\mathbf{U}) \sim \mathcal{N}(\alpha\sqrt{N}Le(n); L(1 + \alpha^2(v(n) - 1))). \quad (26)$$

We thus obtain an approximate expression of the power of the robust test:

$$P_D = \Phi \left(\frac{\Phi^{-1}(P_{FA}) + \alpha\sqrt{N}e(n)}{\sqrt{1 + \alpha^2(v(n) - 1)}} \right). \quad (27)$$

Observe that, once again, the power of the test does not depend on the size of the text. More precisely, it does depend indirectly on it given that α can only take a finite number of values, the number of which decreases with the size of the text. For example, if the text is composed of L tokens, $\alpha \in \{0, 1/L, \dots, 1 - 1/L, 1\}$.

E. Experimental running time

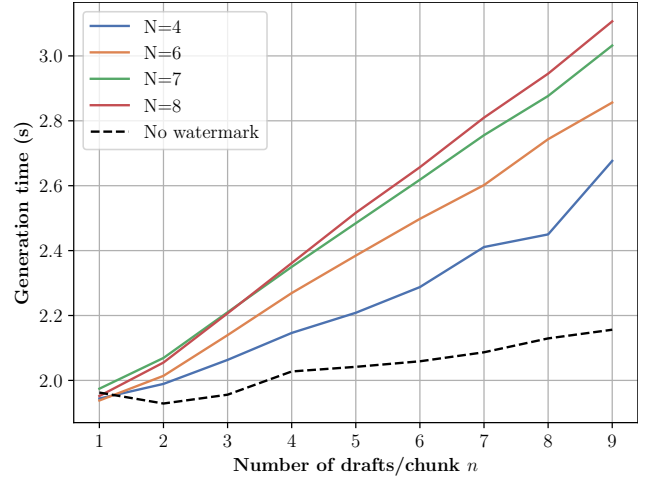


Figure 10: Running time in seconds of WaterMax as a function of the number of chunks N and the number of drafts/chunk n for texts of 64 tokens using sampling on a Nvidia A40.

F. Further experimental results

For all experiments in these supplementary materials, we used the three MMW tasks as defined in (Piet et al., 2023), namely:

- generating 100 fictional news articles,
- generating 100 reports on well-known books,
- generating 96 stories given a synopsis.

Every watermark algorithm is applied on a LLM working at temperature 1.0 with nucleus sampling using the top 95% token probabilities. The maximum text size is fixed at 1024 tokens. The window size is fixed at 4 for every algorithm. For both the Distribution shift and Exponential algorithms, we use the implementation from (Fernandez et al., 2023). Our code to replicate the benchmark is available on Github.

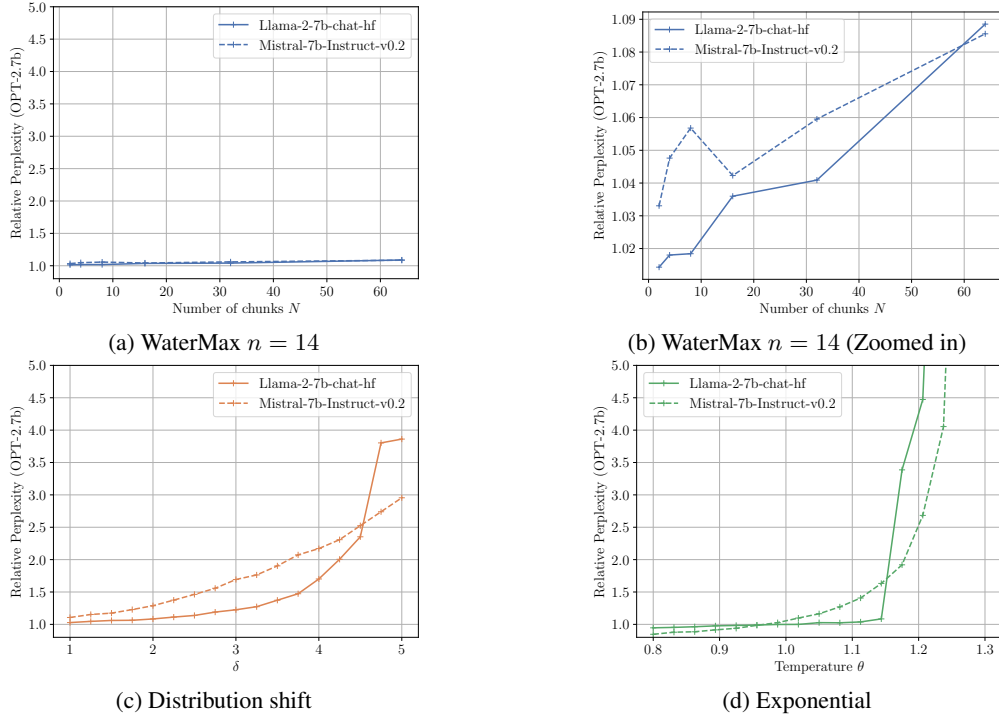


Figure 11: Relative perplexity of each of the studied watermarks using OPT-2.7b as the oracle model. Note that perplexity was constant in n for WaterMax, hence we only provide results for the highest n studied.

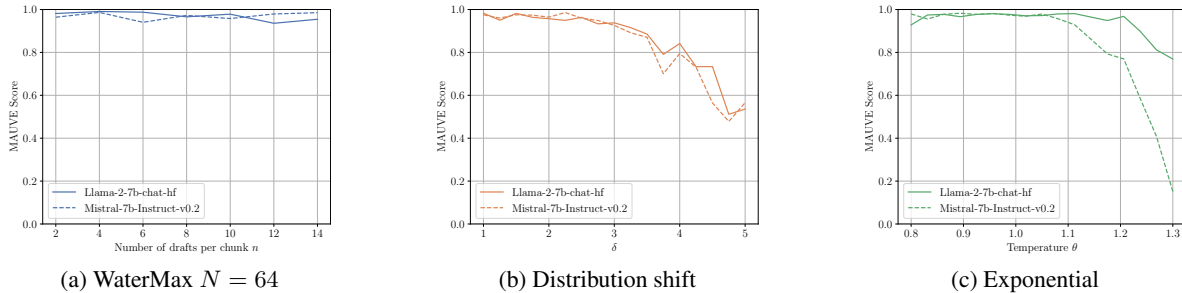


Figure 12: MAUVE score as a function of watermark parameters for two different LLMs.

F.1. Quality

We herein provide further results regarding the impact of WaterMax on text quality compared to the state-of-the-art. We show in Figure 11 the perplexity of each watermark scheme as a function of their parameters. Observe that perplexity seems to stay constant for WaterMax contrary to other algorithms. In practice, we could not find a practical n for which perplexity increased significantly. On the other hand, it does increase for increasing N , albeit extremely slowly compared to other algorithms (see the zoomed in figure).

In Figure 12 we do a similar experiment but using the MAUVE metric (Pillutla et al., 2021). The same conclusions as for perplexity can be made except this time we

never observe a significant deviation from 1 when using WaterMax. Since MAUVE is a lot noisier than perplexity, we favored the latter for comparing with other schemes.

F.2. Detectability

We herein provide further results regarding the detectability of WaterMax compared to the state-of-the-art.

In order to provide a better understanding of the trade-off between quality and detectability for each algorithm, we show in Figure 13 the false-positive rate of the detector for a power of 50% as a function of the perplexity using OPT-2.7b as an oracle. We show the results for two different LLMs: Llama-2-7b-chat and Mistral-7b-Instruct-v0.2. If we look at Llama-2's results, we observe that WaterMax

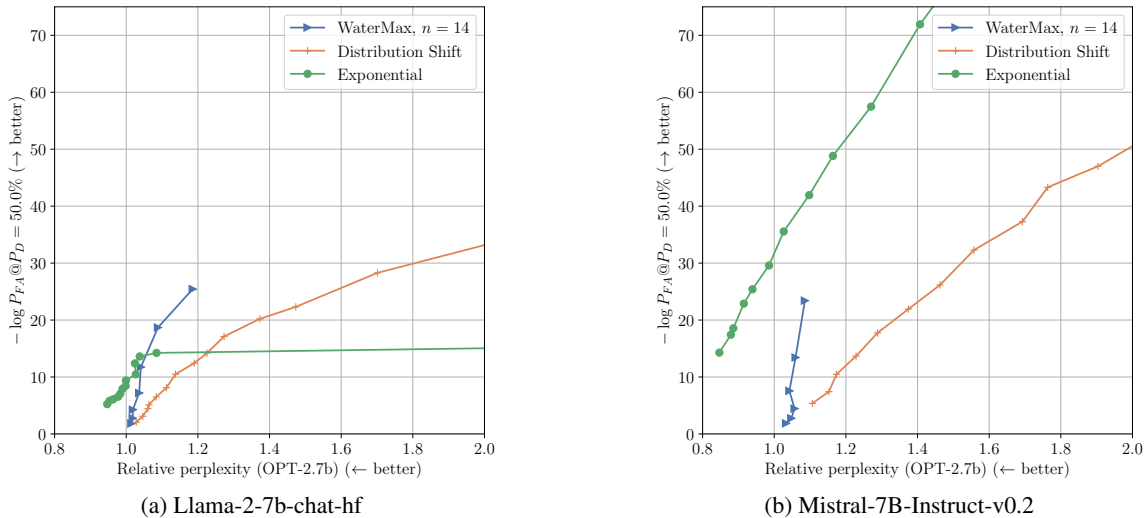


Figure 13: (log) Median false-positive rate as a function of relative perplexity for different watermarking schemes. Note that the relative perplexity for the Exponential scheme can get lower than 1 due to the temperature of the watermark generator being lower than the temperature used to generate the original text.

allows to obtain far better false-positive rates with a minimal impact on quality, with the other algorithms struggling to reach these performances except by substantially increasing the perplexity. Note that the Exponential scheme can go below a relative perplexity of 1 since it directly modify the temperature of the LLM to tune its strength. This can give it an “unfair” advantage since we could similarly improve the performance of both our scheme and the Distribution shift by increasing the temperature which would increase the entropy of the token distribution. Despite this advantage, the Exponential scheme performance stays far below both schemes. However, if we look at the performance for Mistral, this is reversed. Now the Exponential scheme can attain an extremely low false-positive rate even with a temperature close to 1. Our scheme still largely outperforms Distribution shift for quality loss close to 0% but necessitates the use of a high number of chunks to equalize the performance of the Exponential scheme.

This shows the high impact of the LLM on watermark schemes: the three schemes are dependent on the entropy of token distributions to perform well. The Distribution shift and Exponential schemes are extremely sensitive to low entropy distributions since they rely watermark “token by token”, hence the large variations of performance between Llama-2 (lower entropy model) and Mistral (higher entropy model) for the Exponential scheme. On the other hand, WaterMax is far more resilient since it better utilizes the entropy by working on chunks of tokens. As an example, the false positive rate of the Exponential scheme is almost divided by two between Llama-2 and Mistral at temperature 1 whereas our scheme only loses approximately 20% at $N = 64$. Note that the higher the number of chunks N ,

the fewer tokens per chunks and hence the less efficient our scheme becomes.

In Figure 14-16 we provide the false-positive rate of the detector for a power of 50% as a function of the size of the text. This is close to the “watermark size” defined in (Piet et al., 2023) but allows a better overview of the dependency of the watermarks on the text size.

F.3. Robustness

In Section 7 of this paper, we followed (Piet et al., 2023) regarding the measurement of the robustness of a watermark. Even though their method allows to summarize robustness under a single value, it does not tell the whole story since it is computed only for a specific false-alarm rate (2% in their case) and because it does not take into account the original quality of the watermarked text. Indeed, a direct consequence of the tamper-resistance as defined in (Piet et al., 2023) is that one can make a watermark more tamper-resistant by simply increasing its strength. It thus makes little sense to compare algorithms’ tamper-resistance at different quality regimes. Furthermore we found that some attacks that receives a high rating by Llama-2 actually substantially alter the readability of the text. In particular, the Typos-0.1 attacks, which randomly inserts typos in almost every word in the text, makes the resulting text barely legible, yet the attacked texts still obtain a Llama-2 rating within 90% of the of the original watermarked text.

For all these reasons, we report results for individual attacks and for schemes working at a similar relative perplexity of 1.10 in Figure 17-18. Here the story is quite different than the one told using the tamper-resistance metric. If we

look at the absolute performance of the watermarks, they do not differ from the results obtained on detectability with no attacks: Distribution Shift performs the worse at this perplexity regime whereas the WaterMax ($N = 64$) and Exponential schemes rankings depend on the LLM used. On the other hand, if we look at the watermark performance relative to the case where not attack is performed, every watermark seems to perform approximately the same.

This can be explained by leveraging the model presented in Section 5. Recall that any attack has the same impact on a watermarked text: changing one token modifies up to h p -values such that they are distributed under \mathcal{H}_0 instead of \mathcal{H}_1 . Under this model, we can simulate any attack by randomly modifying $(1 - \alpha)\%$, $0 \leq \alpha \leq 1$ of the scores. We can then plot the relative loss of power of the detector as a function of α to study the robustness of the scheme to attacks. Note that this analysis is general in the sense that it does not depend on the existence of an attack at a given α which still results in a text with sufficient quality. We believe the role of the watermark designer is to ensure the highest possible detectability of watermark whatever the strength of the attack; the design of attacks preserving text quality is the burden of the attacker. An analysis of the robustness of a watermark should thus be **comprehensive**, providing the performance of the watermark under any possible type of attacks, existing or not, and **independent of text quality**. We plot the average curves for each watermark in Figure 19. As can be observed, both WaterMax and Distribution Shift have identical robustness for $N = 64$. WaterMax gets slightly more robust for low $(1 - \alpha)$ by lowering N . However, under this analysis, the Exponential scheme is shown to be the most robust scheme, slightly outperforming both WaterMax and Distribution Shift for both Llama-2 and Mistral.

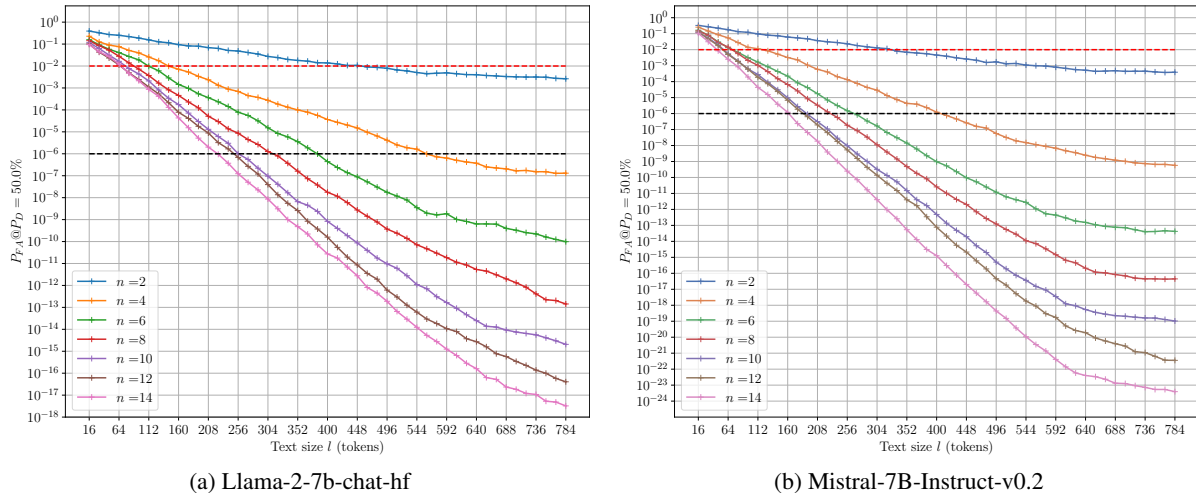


Figure 14: Median false-positive rate as a function of text size in token for the **WaterMax** scheme for $N = 64$. Due to the text size not necessarily reaching 1024 tokens, the average “effective” N is actually equal to 41.

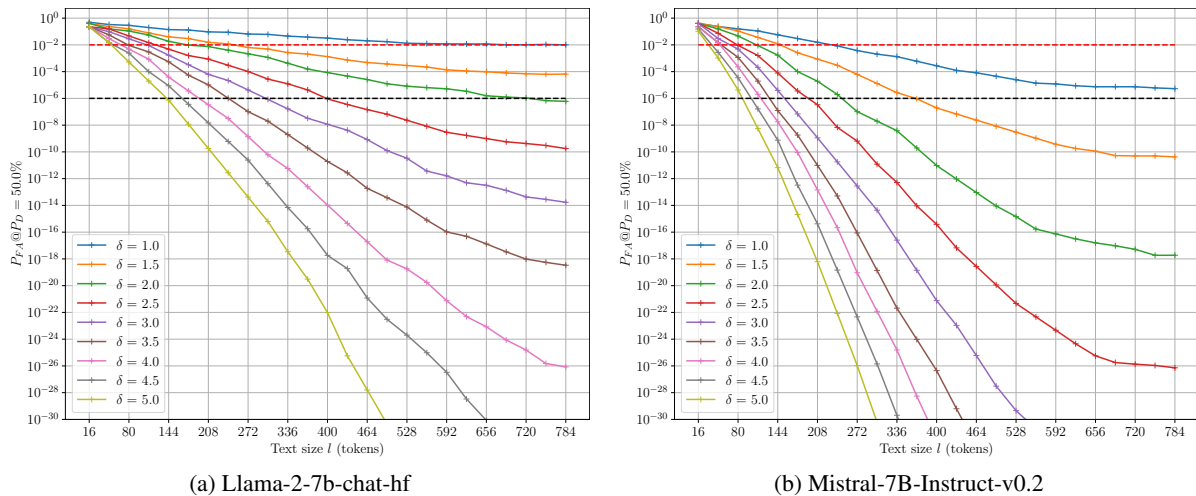


Figure 15: Median false-positive rate as a function of text size in token for the **Distribution Shift** scheme.

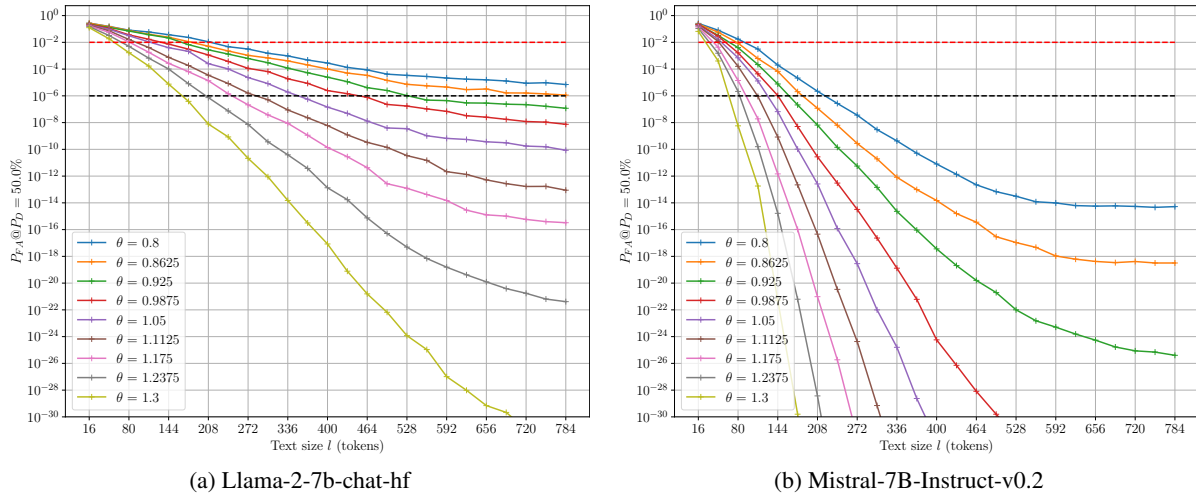


Figure 16: Median false-positive rate as a function of text size in token for the **Exponential** scheme.

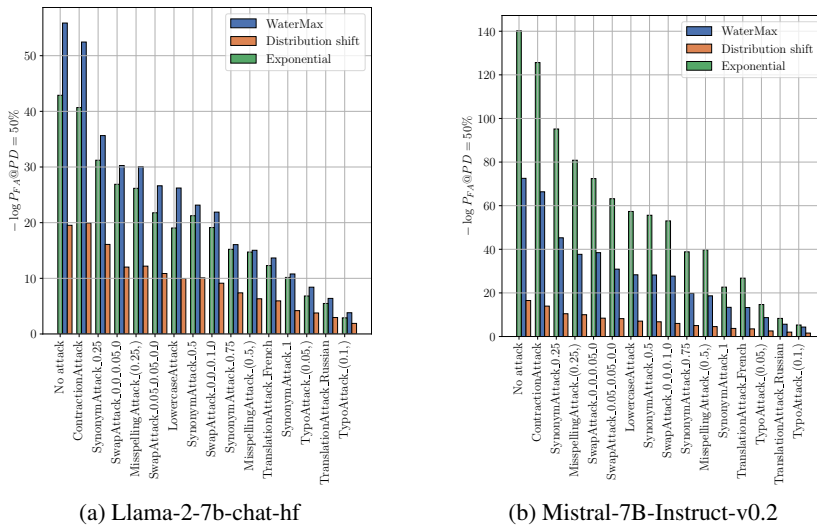


Figure 17: Median false-positive rate as a function of attack on the text. The results are given for watermark parameters leading to a relative perplexity of 1.10.

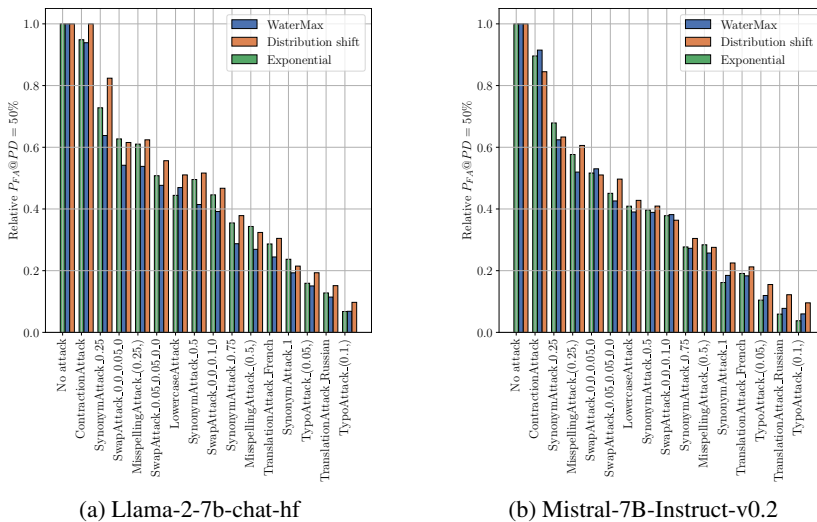


Figure 18: Median false-positive rate as a function of attack on the text relative to the Median false-positive rate when no attack is performed. The results are given for watermark parameters leading to a relative perplexity of 1.10.

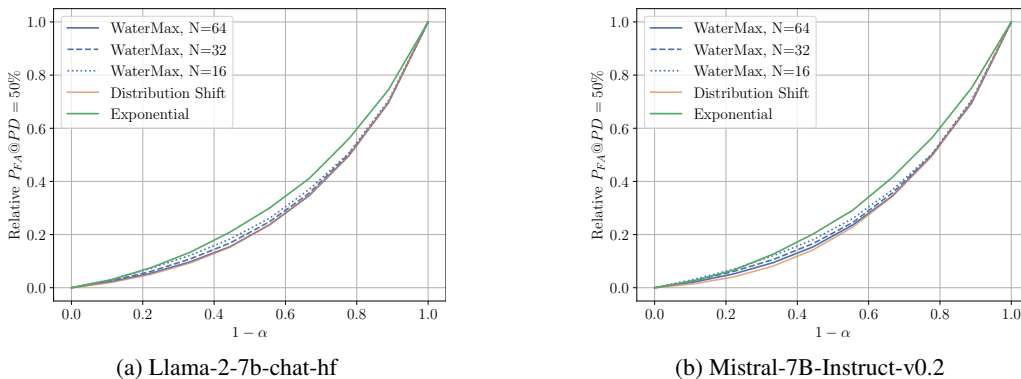


Figure 19: Median false-positive rate as a function of the ratio of modified token scores ($1 - \alpha$). For each watermarking scheme, the curves are averaged for all studied parameters in Figure 14-16.